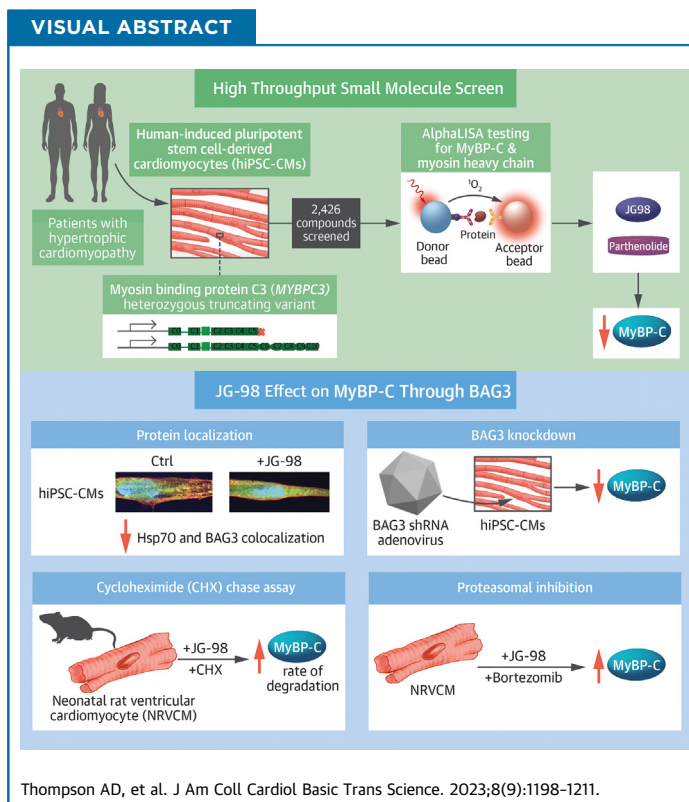


ORIGINAL RESEARCH - PRECLINICAL

# An Unbiased Screen Identified the Hsp70-BAG3 Complex as a Regulator of Myosin-Binding Protein C3



Andrea D. Thompson, MD, PhD,<sup>a</sup> Marcus J. Wagner, PhD,<sup>b</sup> Juliani Rodriguez,<sup>c</sup> Alok Malhotra,<sup>c</sup> Steve Vander Roest, MS,<sup>d</sup> Ulla Lilienthal, MS,<sup>a</sup> Hao Shao, PhD,<sup>e</sup> Mathav Vignesh,<sup>c</sup> Keely Weber,<sup>c</sup> Jaime M. Yob, MS,<sup>b</sup> Benjamin L. Prosser, PhD,<sup>f</sup> Adam S. Helms, MD, MS,<sup>a</sup> Jason E. Gestwicki, PhD,<sup>e</sup> David Ginsburg, MD,<sup>g,h,i,j,k</sup> Sharlene M. Day, MD<sup>b</sup>



From the <sup>a</sup>Department of Internal Medicine, Division of Cardiovascular Medicine, University of Michigan, Ann Arbor, Michigan, USA; <sup>b</sup>Department of Internal Medicine, Division of Cardiovascular Medicine and Cardiovascular Institute, University of Pennsylvania, Philadelphia, Pennsylvania, USA; <sup>c</sup>Department of Internal Medicine, Division of Cardiovascular Medicine, University of Michigan, Ann Arbor, Michigan, USA; <sup>d</sup>Center for Chemical Genomics, Life Sciences Institute, University of Michigan, Ann Arbor, Michigan, USA; <sup>e</sup>Institute for Neurodegenerative Diseases and Department of Pharmaceutical Chemistry, University of California San Francisco, San Francisco, California, USA; <sup>f</sup>Department of Physiology, University of Pennsylvania, Philadelphia, Pennsylvania, USA; <sup>g</sup>Department of Internal Medicine, University of Michigan, Ann Arbor, Michigan, USA; <sup>h</sup>Department of Human Genetics, University of Michigan, Ann Arbor, Michigan, USA; <sup>i</sup>Department of Pediatrics, University of Michigan, Ann Arbor, Michigan, USA; <sup>j</sup>Howard Hughes Medical Institute, Chevy Chase, Maryland, USA; and <sup>k</sup>The Life Sciences Institute, University of Michigan, Ann Arbor, Michigan, USA.

## SUMMARY

Variants in the gene myosin-binding protein C3 (*MYBPC3*) account for approximately 50% of familial hypertrophic cardiomyopathy (HCM), leading to reduced levels of myosin-binding protein C3 (MyBP-C), the protein product made by gene *MYBPC3*. Elucidation of the pathways that regulate MyBP-C protein homeostasis could uncover new therapeutic strategies. Toward this goal, we screened a library of 2,426 bioactive compounds and identified JG98, an allosteric modulator of heat shock protein 70 that inhibits interaction with Bcl-2-associated athanogene (BAG) domain chaperones. JG98 reduces MyBP-C protein levels. Furthermore, genetic reduction of BAG3 phenocopies treatment with JG-98 by reducing MYBP-C protein levels. Thus, an unbiased compound screen identified the heat shock protein 70-BAG3 complex as a regulator of MyBP-C stability. (J Am Coll Cardiol Basic Trans Science 2023;8:1198-1211)  
© 2023 The Authors. Published by Elsevier on behalf of the American College of Cardiology Foundation. This is an open access article under the CC BY-NC-ND license (<http://creativecommons.org/licenses/by-nc-nd/4.0/>).

**H**ypertrophic cardiomyopathy (HCM) is a genetic cardiomyopathy characterized by left ventricular hypertrophy. Patients can experience a variety of adverse cardiovascular outcomes, including left ventricular outflow tract obstruction, heart failure, arrhythmias, and premature death.<sup>1</sup> Cardiac sarcomere genes are the primary genetic basis of HCM, with variants in the gene myosin-binding protein C3 (*MYBPC3*) accounting for approximately 50% of familial cases.<sup>2</sup>

Significant progress has been made in defining the disease mechanism underlying HCM.<sup>3</sup> More than 90% of *MYBPC3* variants are known to create premature stop codons,<sup>4</sup> which are commonly referred to as “truncating variants.” The mutant messenger RNA and protein produced by these variants is rapidly cleared from the cell,<sup>5-7</sup> and mutant myosin-binding protein C3 (MyBP-C), the protein product made by gene *MYBPC3*, is not detectable in cellular lysate.<sup>7</sup> This leads to haploinsufficiency of wild-type (WT) MyBP-C, with levels reduced by approximately 40% in human HCM myectomy tissue.<sup>7-10</sup> Viral delivery of *MYBPC3* prevents and reverses disease phenotypes in both animal and cellular models of disease.<sup>11-14</sup> However, in both human induced pluripotent stem cell-derived cardiomyocytes (iPSC-CMs) and mouse models, a single allelic pathogenic variant is not sufficient to consistently cause disease phenotypes or haploinsufficiency.<sup>8,15</sup> This result suggests that compensatory mechanisms could be exploited to restore WT MyBP-C levels in patients. However, the pathways that regulate expression, folding, trafficking, and/or turnover of MyBP-C remain incompletely defined.

Toward this goal, we developed a high-throughput screen using iPSC-CMs derived from a patient with HCM carrying an *MYBPC3* pathogenic variant. A library of biologically active small molecules was screened to identify those that alter MyBP-C protein levels. From this screen, we identified the heat shock protein 70 (Hsp70)-Bcl-2-associated athanogene 3 (BAG3) complex as a critical regulator of MyBP-C homeostasis, suggesting that stabilizing the Hsp70-BAG complex could be a therapeutic target for HCM caused by *MYBPC3* loss-of-function variants.

## METHODS

### INDUCED PLURIPOTENT STEM CELL-DERIVED

**CARDIOMYOCYTES.** iPSCs used in this study are from 4 control lines (Ctrl 1,2,3,4), 3 patient-derived lines obtained from patients with HCM who were genotype positive for a pathogenic truncating variant in *MYBPC3* (*MYBPC3* Patient1,2,3) and a gene-edited iPSC homozygous *MYBPC3* knockout line (*MYBPC3* [-/-]) (Supplemental Table 1, Supplemental Figure 1).<sup>15-19</sup> Details regarding stem cell maintenance, cardiomyocyte production, and cell culture are provided in the Supplemental Appendix. The iPSC-CMs used in our screen showed >90% purity by immunostaining for  $\alpha$ -actinin (Supplemental Figure 2). Mass spectrometry, performed as described further in the Supplemental Appendix, on *MYBPC3* Patient1 iPSC-CM cellular lysate confirms that *MYBPC3* is the only *MYBPC* isoform present (Supplemental Table 2).

## ABBREVIATIONS AND ACRONYMS

- BAG** = Bcl-2-associated athanogene
- BAG3** = Bcl-2-associated athanogene 3
- EC<sub>50</sub>** = half maximal effective concentration
- HCM** = hypertrophic cardiomyopathy
- Hsp70** = heat shock protein 70
- iPSC-CM** = induced pluripotent stem cell-derived cardiomyocyte
- MyBP-C** = myosin-binding protein C3, the protein product made by gene *MYBPC3*
- MYBPC3** = the gene myosin-binding protein C3
- MYH** = myosin heavy chain
- PTL** = parthenolide
- shRNA** = small hairpin RNA
- WT** = wild-type

The authors attest they are in compliance with human studies committees and animal welfare regulations of the authors' institutions and Food and Drug Administration guidelines, including patient consent where appropriate. For more information, visit the [Author Center](#).

Manuscript received March 6, 2023; revised manuscript received April 17, 2023, accepted April 18, 2023.

A detailed method section is provided in the [Supplemental Appendix](#). This includes the high-throughput Alpha-LISA screening assay ([Supplemental Figures 3 to 5](#)), details regarding compound libraries ([Supplemental Table 3](#)), cell toxicity testing, immunofluorescence, contractility measurements, cycloheximide chase analysis, adenovirus treatment, and Western blot analysis.

**STATISTICAL ANALYSIS.** Statistical analysis was performed by using GraphPad Prism software (GraphPad Prism 8 Software). Kruskal-Wallis nonparametric one-way analysis of variance with Dunn's post hoc test for multiple pairwise comparisons were used for comparisons. *P* values <0.05 were considered statistically significant. Data are reported as mean ± SEM. Linear regression and nonlinear regressions were performed in GraphPad Prism (GraphPad Prism 8 Software). Linear regression was performed for results obtained by testing serial dilutions of cellular lysate in the MyBP-C and myosin heavy chain (MYH) Alpha-LISA assay; goodness of fit was evaluated with coefficients of determination ( $R^2$ ). Concentration-response curves were analyzed by performing an inhibitor vs response, variable slope nonlinear regression. Cycloheximide chase assay data were analyzed by using a one-phase decay nonlinear regression. Parameters obtained from these nonlinear regressions, such as the half-maximal effective concentration ( $EC_{50}$ ) and half-life, are reported as least squares mean with 95% CI. If constraints were used in the nonlinear regressions, this is indicated in the table or figure legends. Finally, the degree of co-localization of Hsp70 and BAG3 was analyzed for immunofluorescence images in patterned cardiomyocytes using NIS-Elements AR Analysis version 5.30.03 software (Nikon, Instruments Inc). Pearson's correlation is reported and describes the extent of overlap between the Hsp70 and BAG3 immunofluorescence signals within the cytosol of a single cardiomyocyte. Additional details regarding data analysis are provided within the [Supplemental Appendix](#).

**STUDY APPROVAL.** All animal studies were conducted with the approval of the University of Michigan Institutional Animal Care and Use Committee (PRO00009438). All patient samples were collected with the approval of the University of Michigan Institutional Review Board, and all subjects gave written informed consent (HUM00041413, HUM00052165).

## RESULTS

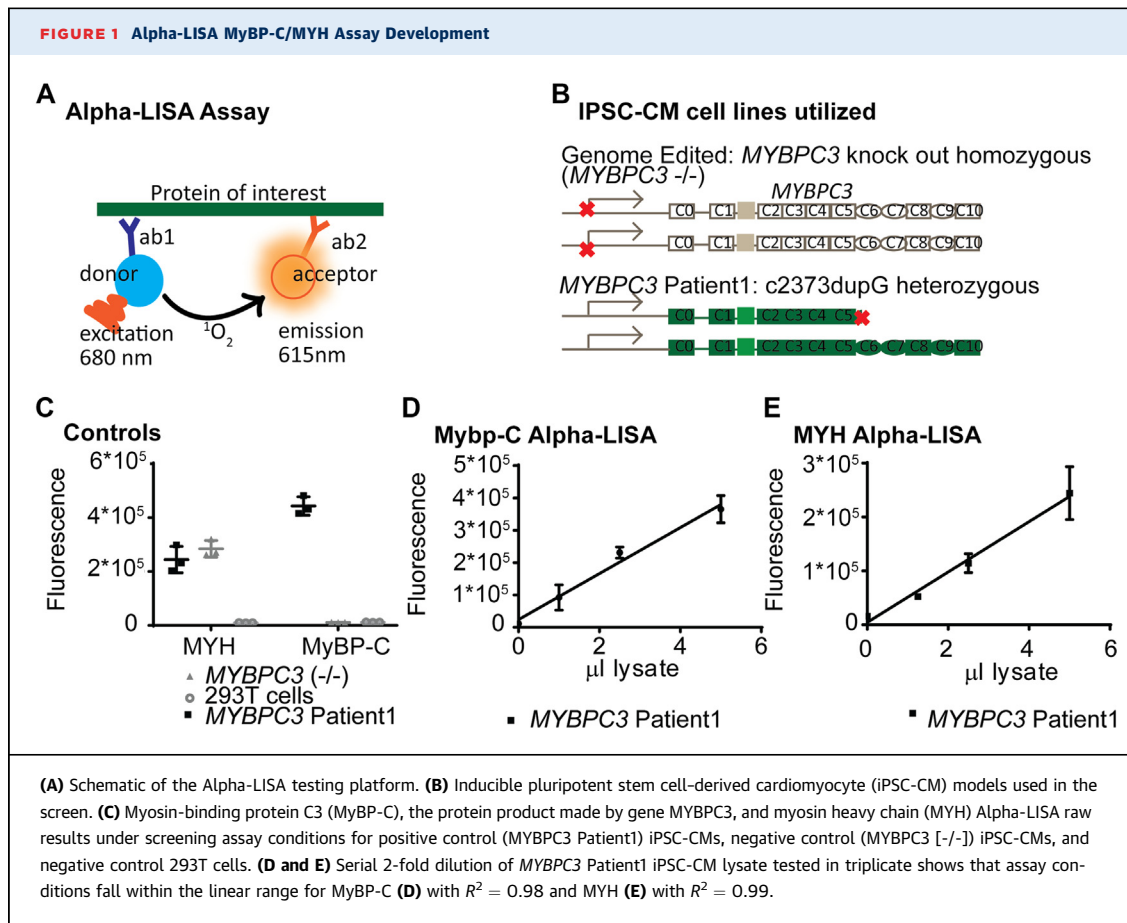
**HIGH-THROUGHPUT SCREENING.** To identify pathways that regulate MyBP-C stability, we envisioned screening a collection of bioactive small molecules in

a cell-based model. To enable this screen, a no-wash, homogenous immunoassay technology (Alpha-LISA, PerkinElmer) was used. We developed an Alpha-LISA assay quantifying MyBP-C, within a cellular lysate sample, using 2 antibodies linked to donor and acceptor beads ([Figure 1A](#), [Supplemental Table 4](#)). In choosing cells for this screen, a well-characterized iPSC cell line derived from a patient with HCM was used to generate CMs (*MYBPC3* Patient1 [+/*c.2373dupG*])<sup>15-17</sup> ([Figure 1B](#)). Another key design in our screen was the simultaneous measurement of MYH, using antibodies that detect  $\alpha$ MYH and  $\beta$ MYH via a parallel Alpha-LISA. This feature allowed us to control for sarcomere content in each well and focus on compounds that modulated MyBP-C via reporting of the MyBP-C/MYH ratio. Both MyBP-C and MYH Alpha-LISA exhibited an excellent signal-to-noise ratio and a linear relationship between the Alpha-LISA signal and total protein concentration when testing *MYBPC3* Patient1 cellular lysates ([Figures 1C to 1E](#)).

Using a primary endpoint of MyBP-C/MYH ratio, we screened 2,426 compounds representing 2,400 U.S. Food and Drug Administration-approved molecules or known bioactive compounds and a curated subcollection of 26 molecules that target known MyBP-C-interacting proteins. In this screen, in-plate controls were used to allow determination of the assay robustness, yielding an average in-plate Z-factor of 0.66. In-plate Z-factors ranged from 0.44 to 0.83 and are reported in [Supplemental Figure 6](#). Using a criterion of 3 SDs from the controls, 241 (9.9%) of 2,426 hit compounds that decreased MyBP-C/MYH levels were identified ([Figure 2](#)). Also identified were 29 (1.2%) of 2,426 hit compounds that increased MyBP-C/MYH levels ([Supplemental Table 5](#)).

**VALIDATING SCREENING HITS.** In any high-throughput screening campaign, it is important to establish reproducibility of initial hits ([Figure 2A](#)). A detailed description of the validation process is provided in the [Supplemental Appendix](#). No compounds that increased MyBP-C/MYH protein levels showed activity after repeat testing. Fifty-two compounds that decreased MyBP-C/MYH protein levels exhibited activity after repeat testing ([Supplemental Table 6](#)).

Secondary assays were next used to focus on the most robust hits. First, we analyzed MyBP-C and MYH Alpha-LISA separately and selected compounds that reduced MyBP-C levels without significantly altering MYH levels ([Figure 2B](#), [Supplemental Tables 7 and 8](#), [Supplemental Figure 7](#)). Finally, 14 hits that met the aforementioned criteria were evaluated in a counter-screen for cytotoxicity ([Supplemental Figure 8](#), [Supplemental Table 9](#)). Compounds that exhibited

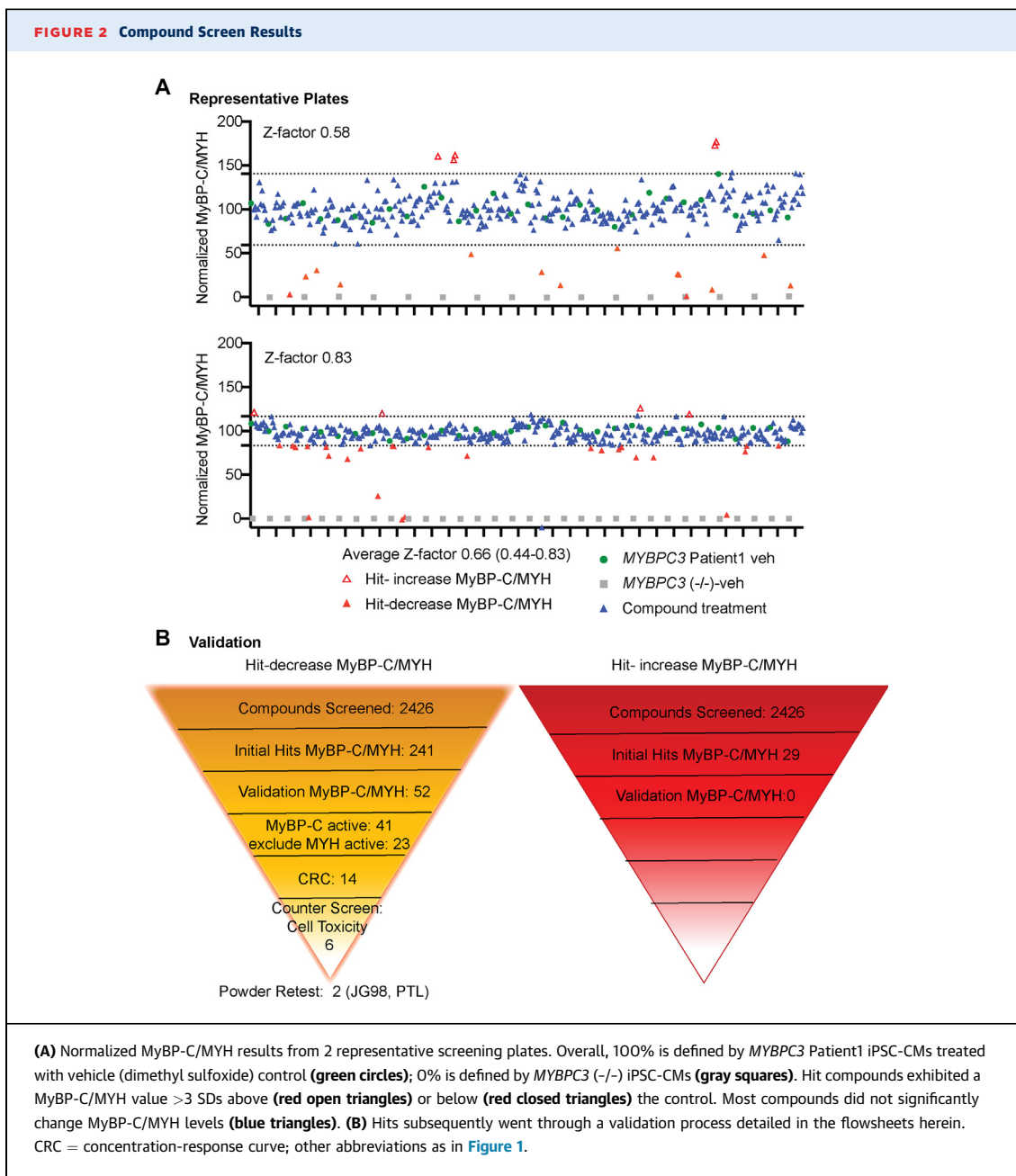


toxicity with an  $EC_{50} \leq 60 \mu M$  were excluded. After these steps, 6 compounds were left that decreased MyBP-C/MYH protein levels by decreasing MyBP-C protein levels with no significant effect on MYH protein levels or cellular toxicity.

To further evaluate these 6 compounds, we re-ordered fresh powders and tested them in the Alpha-LISA assay (Supplemental Table 10). From these experiments, only JG98 and parthenolide (PTL), a sesquiterpene lactone, retained activity (Figure 3A, Supplemental Figure 9). Specifically, JG98 exhibited an  $EC_{50}$  of 12.1  $\mu M$  (95% CI: 8.3-18.0). JG98 also decreased MYH, but at a higher concentration, with an  $EC_{50}$  of 43.8  $\mu M$  (95% CI: 29.1-68.4). PTL exhibited an  $EC_{50}$  of 43.8  $\mu M$  (95% CI: 29.1-68.4), with no significant activity noted in the MYH assay. This activity was maintained in a control line and 2 other patient-derived lines (Figure 3B, Table 1). The ability of PTL and JG98 to reduce MyBP-C protein levels was confirmed in an orthogonal Western blot analysis on whole cellular lysates run on sodium dodecyl sulfate denaturing gels (Supplemental Figure 10).

PTL is a natural product that has a variety of reported biologic activities, including inhibition of histone deacetylase 1, modulation of nuclear factor kappa B and Hsp70, and reduction of deetyrosinated  $\alpha$ -tubulin.<sup>20-22</sup> JG98 is an allosteric modulator of Hsp70, which is known to inhibit Hsp70 binding to an important class of co-chaperones, the BAG domain proteins.<sup>23,24</sup> Given that sex-associated differences have been observed in BAG domain protein-related diseases and in BAG domain protein localization,<sup>25,26</sup> we proceeded to test JG98 in an additional female and male control line. No significant differences in activity were observed across cell lines (Figure 3C). Thus, these screens identified 2 compounds that affected MyBP-C levels.

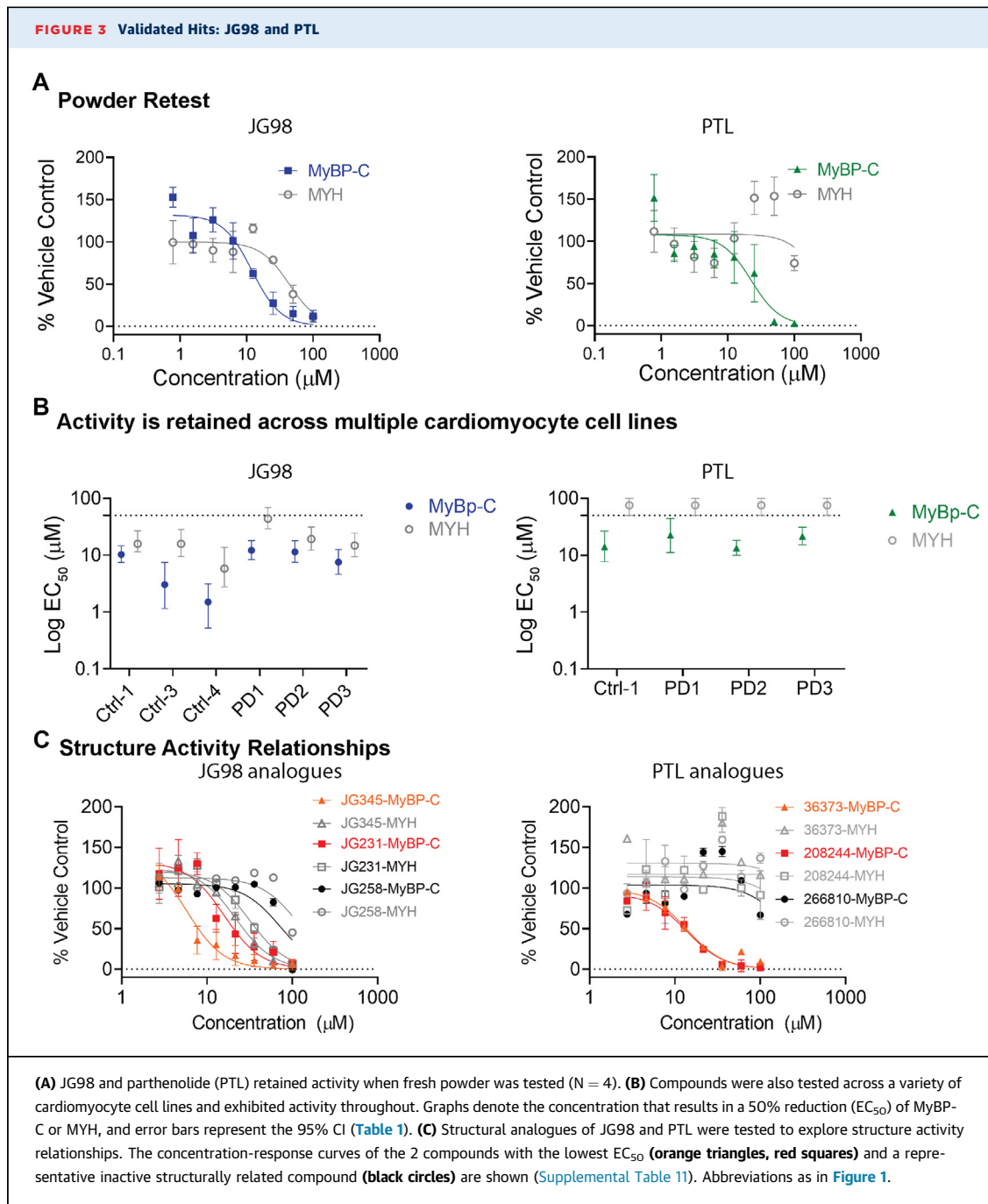
**STRUCTURE ACTIVITY RELATIONSHIPS.** To gain further insight into the validated hits, we tested analogues that are structurally related to JG98 and PTL (Figure 2C, Supplemental Table 10). Our goal was to understand whether the expected structure activity relationship would correlate with the observed effects on MyBP-C abundance. In the



Alpha-LISA, we found that PTL-related compounds containing the reactive epoxide moiety were active, but those lacking the epoxide were inactive (Supplemental Table 10). One exception was eunicin, although this compound also reduced MYH levels. These findings are consistent with the known biologic activity of PTL, which uses a covalent mechanism of action, driven by the reactivity of the epoxide moiety.<sup>20</sup>

JG98 is part of a medicinal chemistry campaign of  $\geq 400$  compounds to develop Hsp70-BAG inhibitors.<sup>23,27,28</sup> We found that the activity of the analogues tracked with their known potency in other systems. For example, JG258 is a structurally related compound without activity against Hsp70, and it did not reduce MyBP-C protein levels (Figure 3C).<sup>27</sup> Likewise, analogues such as MKT-077, YM-1, and YM-8 are known to have reduced activity against Hsp70,





compared with JG98, and they also did not reduce MyBP-C protein levels<sup>29,30</sup> (Supplemental Table 11). Conversely, more potent analogues such as JG231 and JG345 reduced MyBP-C protein levels at a lower concentration than JG98.<sup>27</sup> Together, these results support the idea that the Hsp70-BAG system is important for MyBP-C stability.

**MECHANISM OF ACTION FOR PTL IS LIKELY INDEPENDENT OF DETYROSINATION OF  $\alpha$ -TUBULIN.** The most well-

studied activity of PTL in cardiomyocytes is its ability to decrease the amount of detyrosinated  $\alpha$ -tubulin.<sup>21</sup> Detyrosinated  $\alpha$ -tubulin is a post-translational modification generated by carboxypeptidases (vasohibin 1/2-small vasohibin binding protein),<sup>31,32</sup> and this process is reversed by tubulin tyrosine ligase.<sup>33</sup> Thus, it is possible that PTL could reduce MyBP-C through this pathway. To test this possibility, we treated the cells with adenovirus to

**TABLE 1 Testing PTL and JG98 in Multiple Cell Lines**

	MyBP-C				MYH				N
	EC <sub>50</sub> (μM)	95% CI	Top % Vehicle <sup>a</sup>	95% CI	EC <sub>50</sub> (μM)	95% CI	Top % Vehicle	95% CI	
<b>JG98</b>									
Ctrl-1	10.3	7.4-14.6	75	65- 86	15.8	11.4-22.3	107	94-121	5
Ctrl-3	3.02	1.15-7.49	52	33-89	16.7	10.5-29.5	84.3	71-98	4
Ctrl-4	1.5	0.5-3.1	71	43-204	5.8	2.3-13.6	86.9	64-122	4
PD -1 <sup>b</sup>	12.1	8.3-18.0	132	115-150	43.8	29.1-68.4	100	87-113	5
PD-2	11.4	7.5-17.8	94	79-109	19.2	12.2-31.1	142	120-164	7
PD-3	7.5	4.7-12.6	70	57- 85	14.8	9.4-24.4	92	76-110	4
<b>PTL</b>									
Ctrl-1	14.1	7.7-26.5	113	91-138	>50	-	115	104-126	5
PD-1	22.5	11.1-44.2	118	85-131	>50	-	109	91-127	5
PD-2	13.4	9.9-18.2	118	105-131	>50	-	115	107-123	7
PD-3	21.5	15.3-31.0	104	91-116	>50	-	95	-	4

Concentration-response curves were fit using the inhibitor vs response-variable slope nonlinear regression in GraphPad Prism. Half-maximal effective concentration (EC<sub>50</sub>) and Top represent least squares mean estimates from this nonlinear regression model. Constraints included Bottom = 0, hill slope = -2, respectively. <sup>a</sup>Vehicle control is dimethyl sulfoxide. <sup>b</sup>PD refers to the gene myosin-binding protein C3 (*MYBPC3*) patient inducible pluripotent stem cell-derived cardiomyocytes (1,2,3).

increase expression of tubulin tyrosine ligase and, separately, knocked down VASH1 with small hairpin RNA (shRNA). We validated that these manipulations reduced detyrosinated  $\alpha$ -tubulin, as expected (Supplemental Figure 11). However, there was no change in MyBP-C/MYH levels. These results suggest that PTL regulates MyBP-C homeostasis via a mechanism distinct from its known effects on detyrosinated  $\alpha$ -tubulin.

**JG98 IDENTIFIES HSP70-BAG3 AS A KEY REGULATOR OF MYBP-C PROTEIN HOMEOSTASIS.** The current study subsequently focused on understanding the mechanism by which JG98 reduces MyBP-C protein levels. We began by re-evaluating cell toxicity of JG98 and its analogues. Again, we found that these compounds do not exhibit significant toxicity at concentrations that reduce MyBP-C protein levels (Figure 4, Supplemental Table 12). Next, the effect of JG98 on myofilament structure was evaluated (Figure 4, Supplemental Figure 12). A 27.5% reduction was observed in MyBP-C/ $\alpha$ -actinin in cells treated with JG98 compared with vehicle control ( $P < 0.001$ ), with no significant change in cells treated with JG258. Using a blinded scoring system,<sup>34</sup> no change was noted in myofibrillar disarray. Despite this lack of effect on myofibrillar disarray, JG98 treatment inhibited contractility in cardiomyocytes (Supplemental Figure 13).

Structure activity relationships suggest that JG98 reduces MyBP-C via its known activity as an allosteric inhibitor of Hsp70 binding to BAG domain proteins (Figure 3). BAG3 is one of the BAG family of co-

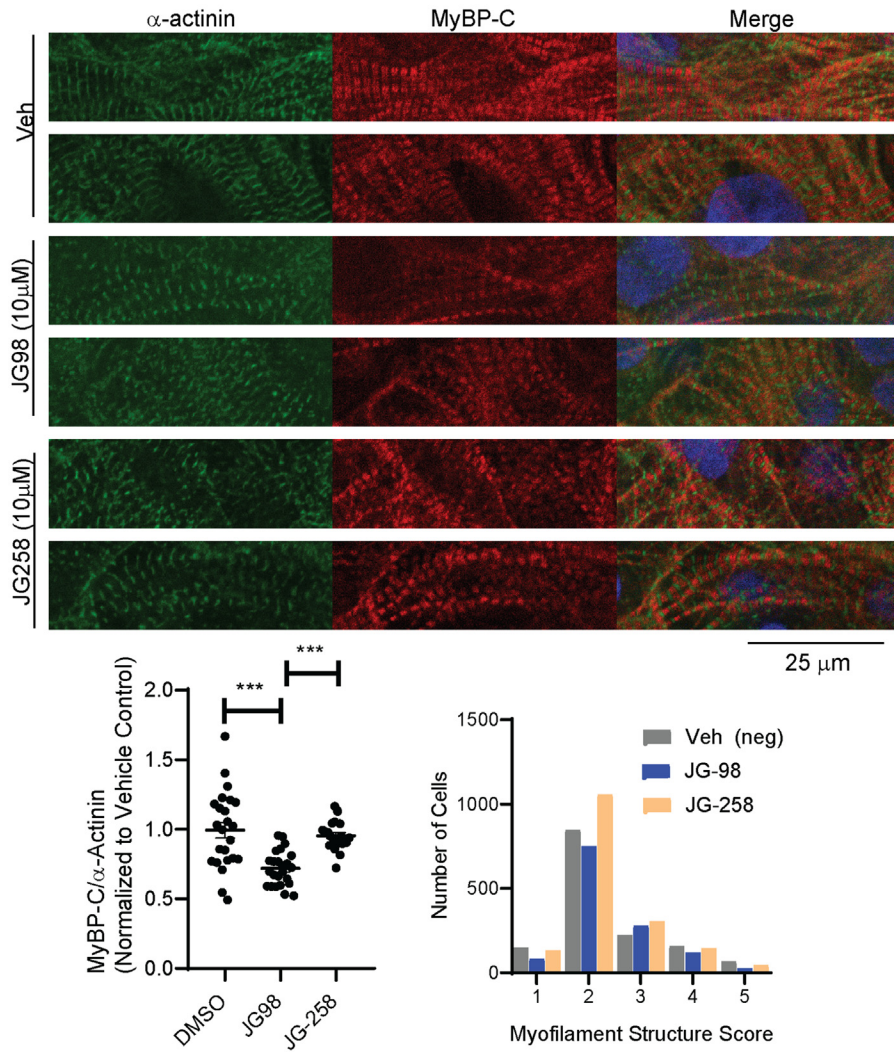
chaperones that is highly expressed in cardiomyocytes and localizes to the sarcomere,<sup>35,36</sup> where it is believed to play a role in the folding and assembly of sarcomere proteins. Thus, we hypothesized that JG98 induces MyBP-C degradation by disrupting the Hsp70-BAG3 interaction (Figure 5A). Consistent with this hypothesis, JG-98 treatment reduced co-localization of Hsp70 and BAG3 by immunofluorescence (Figure 5B). We also showed that shRNA knockdown of BAG3 reduced MyBP-C protein levels (Figure 5C), genocopying the effect of JG98 on MyBP-C. Furthermore, using a cycloheximide chase assay, JG98 treatment was shown to shorten the half-life for WT MyBP-C (Figure 5D). Proteasome inhibition blocked JG98-induced reductions in MyBP-C (Figure 5E). Taken together, these results support a model in which disruption of Hsp70-BAG3 interactions leads to proteasome-dependent degradation of MYBP-C.

## DISCUSSION

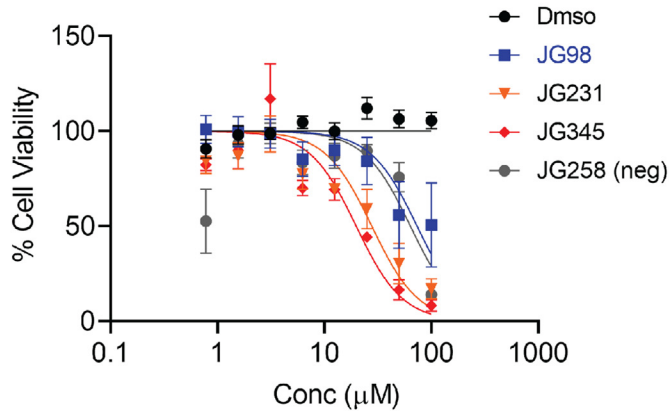
Pathogenic truncating variants in *MYBPC3* lead to HCM by causing haploinsufficiency.<sup>7,9</sup> However, haploinsufficiency and hypercontractility are not consistently observed in published mouse or iPSC-CM models with heterozygous truncating *MYBPC3* variants.<sup>8,15</sup> Our group has shown previously that this compensatory response in iPSC-CMs occurs by slowing the degradation rate of the remaining WT protein.<sup>15</sup> This compensatory mechanism is evidently lost in patients with HCM because tissue levels of WT

**FIGURE 4** JG98 Reduces MyBP-C Protein Levels Without Inducing Toxicity or Disrupting Myofilament Structure

**A** JG-98 reduces MYBP-C/ $\alpha$ -actinin without significantly disrupting myofilament structure



**B** JG98 and analogs do not exhibit significant toxicity at the concentrations which lead to MyBP-C reductions



Continued on the next page



MyBP-C are consistently reduced in myectomy tissue.<sup>7</sup> Thus, identifying the pathways that regulate MyBP-C protein levels is important to understand the processes that may be therapeutically targeted to halt disease progression.<sup>3</sup> Herein, we developed a high-throughput small-molecule screen to identify regulators of MyBP-C protein levels. Two small molecules that reduce MYBP-C protein levels (JG98 and PTL) were identified. JG98 led us to pinpoint the Hsp70-BAG3 axis as a critical and potentially intervenable target to control MyBP-C abundance.

One important product of this work is the development of a robust high-throughput screen in iPSC-CMs. We screened a relatively small library with 2,426 bioactive compounds. We did not identify any immediate therapeutic leads (compounds that increased MyBP-C protein levels). Nonetheless, this work shows the feasibility of our screening approach, which is readily amenable to scale-up. It is our hope that future screens, using larger and more diverse chemical collections, will uncover therapeutic leads that increase MyBP-C protein levels.

The screen did identify 2 compounds (JG98 and PTL) that decrease MyBP-C protein levels. The activity of PTL and JG98 was consistent across multiple iPSC-CM cell lines, showing that activity is not dependent on the genetic background, sex, or batch-specific variables of cardiomyocyte differentiation. Understanding the molecular mechanism by which these compounds reduce MyBP-C levels may uncover pathways that contribute to the development of MyBP-C haploinsufficiency in patients with HCM and lead to the development of novel therapeutic strategies.

PTL contains an epoxide moiety that enables it to make covalent modifications to cysteine amino acids.<sup>20</sup> By testing PTL analogues, we found that the ability to reduce MyBP-C protein levels is dependent on this epoxide. However, the target protein that leads to alterations in MyBP-C protein levels remains unknown. Our results suggest that the activity of PTL on detyrosinated  $\alpha$ -tubulin is not relevant to its activity on MyBP-C, suggesting that other targets must be involved. Given the pleiotropic cellular targets of PTL,<sup>20-22</sup> identification of this target is expected to be

challenging and is outside the scope of the current work.

In contrast, our results with JG98 and its analogues strongly suggest that the Hsp70-BAG complex is important for MyBP-C homeostasis. JG98 reduced steady-state MyBP-C protein levels at concentrations that did not lead to alterations of myofibrillar disarray or significant cellular toxicity. JG98 is known to bind a conserved allosteric site on Hsp70, trapping a conformation that has weak affinity for BAG domain proteins.<sup>30</sup> JG98 has been shown to disrupt Hsp70-BAG domain-binding in a variety of cellular systems, including cardiomyocytes.<sup>27,37</sup> To further evaluate how JG98 leads to MyBP-C protein reduction, we tested a structurally related control that lacks activity against Hsp70, JG258.<sup>27</sup> JG258 did not affect MyBP-C protein levels, showing that the affinity for Hsp70 is critical. Furthermore, compounds with improved affinity for Hsp70 (ie, JG231, JG345) also led to reductions in MyBP-C at lower concentrations.<sup>23,27,28</sup> These results are consistent with JG98, leading to reductions in MyBP-C via its known activity as an allosteric inhibitor of Hsp70-BAG domain interactions.

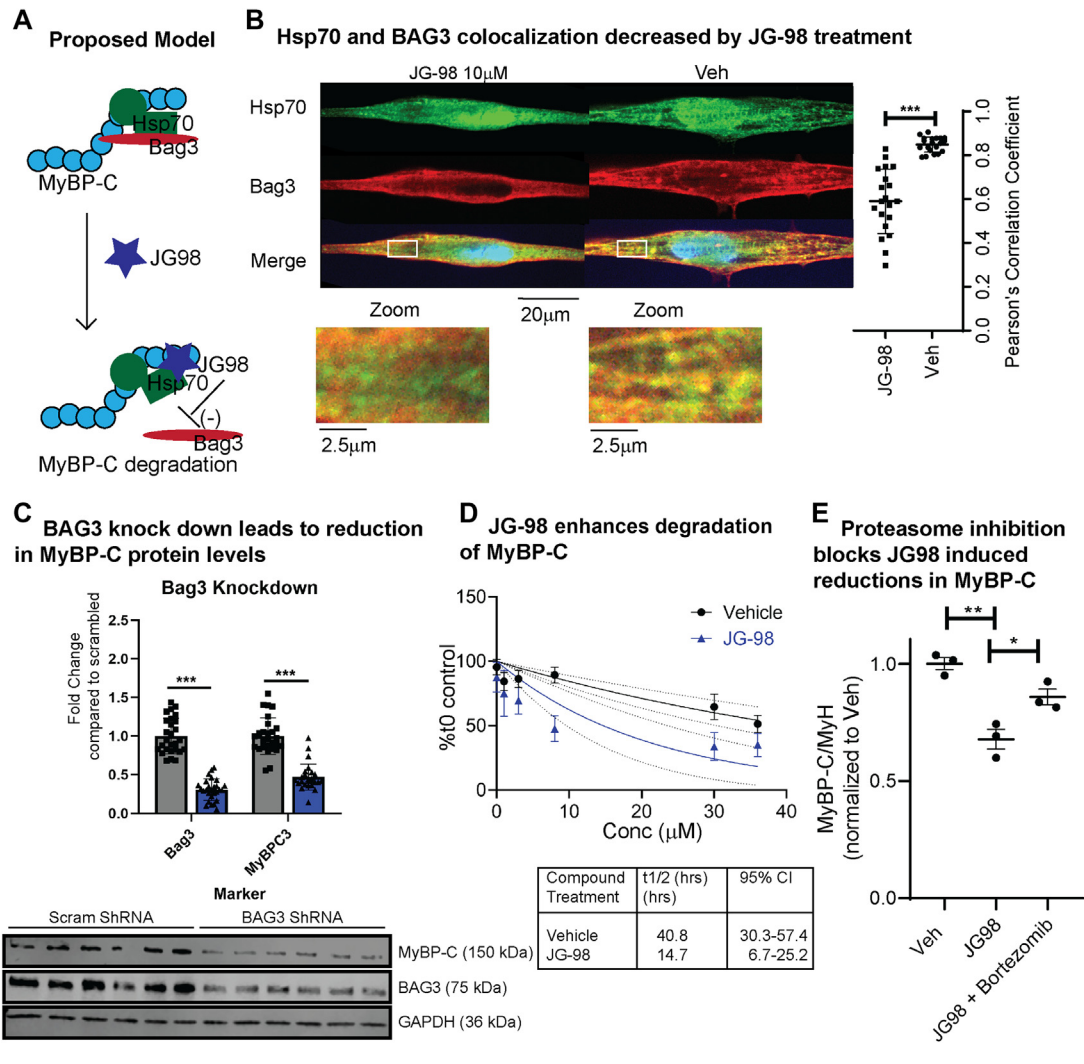
Of note, there are 2 cytosolic isoforms of Hsp70 and 6 BAG proteins.<sup>38</sup> Knockdown of one cytosolic isoform of Hsp70 leads to overexpression of the other and as such did not alter JG98 activity when previously tested.<sup>27,39</sup> Dual knockdown is cytotoxic.<sup>39</sup> Interestingly, our pilot screen also contained other Hsp70 modulators, which were not active (Supplemental Table 3). These compounds, such as 115-7c, are known to bind other sites on Hsp70 and to have distinct effects on other (non-BAG) co-chaperones.<sup>40,41</sup> Thus, these observations suggest that the Hsp70-BAG complex may be the most important Hsp70 co-chaperone interaction for regulation of MyBP-C stability.

We next focused on the importance of BAG3-Hsp70 interaction for several reasons. First, BAG3 localizes to the sarcomere.<sup>26</sup> Second, human genetic studies point to an important role for BAG3 in human cardiomyopathy. Rare loss-of-function variants in BAG3 are associated with dilated cardiomyopathies.<sup>42,43</sup> Furthermore, common BAG3 variants have been

#### FIGURE 4 Continued

(A) Representative images of Ctrl-3 iPSC-CMs with JG98 (10  $\mu$ M), JG258 (10  $\mu$ M), or vehicle control are shown with  $\alpha$ -actinin (green) and MyBP-C (red) (Supplemental Figure 12). Blinded analysis (N = 24) reveals reduced levels of MyBP-C/ $\alpha$ -actinin in JG98 but not in JG258 samples and no significant change in myofibrillar disorder. (B) Cellular toxicity of JG98 and analogues did not exhibit significant toxicity at the concentrations that lead to MyBP-C reductions (Supplemental Tables 9 and 12). \*\*\*P < 0.001. Conc = concentration; DMSO = dimethyl sulfoxide; neg = negative; Veh = vehicle; other abbreviations as in Figure 1.

**FIGURE 5** Disruption of the BAG3-Hsp70 Complex by BAG3 Knockdown or JG98 Treatment Reduces MyBP-C Protein Levels



**(A)** Proposed model: JG98 induces MyBP-C degradation by inhibiting heat shock protein 70 (Hsp70) and Bcl-2-associated athanogene 3 (BAG3) binding. **(B)** Micropatterned Ctrl-3 iPSC-CMs were treated with JG98 (10  $\mu$ M) or vehicle control in duplicate. Representative images of immunofluorescence for Hsp70 (green) and BAG3 (red) and merged images are shown. The extent of co-localization within the cytosol between Hsp70 (green) and BAG3 (red) was measured by using Pearson's correlation for each cell tested. There is less Hsp70 and BAG3 co-localization (lower Pearson's correlation) in cells treated with JG98 than in vehicle control (N = 20). **(C)** A representative Western blot is shown. Ctrl-2 iPSC-CMs were cells treated with an adenovirus at a multiplicity of infection 5 carrying scrambled small hairpin RNA (shRNA) (gray bars, black squares) or BAG3 shRNA (blue bars, black triangles) for 18 hours. Cellular lysates were analyzed 4 days after shRNA treatment (n = 27; 5 biologic replicates). Quantification of Western blots shows significant reduction of BAG3 and MyBP-C. Glyceraldehyde-3-phosphate dehydrogenase (GAPDH) was also used as a loading control. **(D)** Cycloheximide chase assay shows that treatment with JG98 results in more rapid clearance of MyBP-C from neonatal rat ventricular cardiomyocytes compared with vehicle control (DMSO). JG98 was tested at 1  $\mu$ M for 24 hours. The EC<sub>50</sub> of JG98 in neonatal rat ventricular cardiomyocytes is 1.2  $\mu$ M (95% CI, 0.4-3.00). **(E)** Alpha-LISA analysis of MyBP-C/MYH on Ctrl-3 iPSC-CMs treated with vehicle control, JG98 (20  $\mu$ M), or JG98 (20  $\mu$ M) and bortezomib (0.5  $\mu$ M) for 24 hours shows that inhibition of the proteasome blocks JG98-mediated reductions in MyBP-C/MYH. \*P < 0.05, \*\*P < 0.01, \*\*\*P < 0.001. Conc = concentration; t1/2 = half-life; Veh = vehicle; other abbreviations as in Figures 1, 3, and 4.

identified in genome-wide association studies with opposing direction of risk for dilated cardiomyopathies and HCM.<sup>44-46</sup> The effects of these common variants on BAG3 activity and disease pathogenesis

remain unknown. Additional experiments performed here support the hypothesis that Hsp70-BAG3 interactions stabilize MyBP-C (Figure 5A). First, we found that JG98 reduced co-localization of cytosolic

Hsp70 and BAG3 in iPSC-CMs. Furthermore, JG98 shortens the half-life of MyBP-C. Finally, BAG3 knockdown reduces MyBP-C protein levels. Prior work in loss-of-function BAG3 mutants found that these mutants caused the accumulation of other sarcomere proteins within the insoluble fraction of cellular lysates.<sup>47</sup> Thus, we evaluated total MyBP-C protein levels (soluble and insoluble fractions combined) by performing Western blot analysis on whole cell lysate run on sodium dodecyl sulfate denaturing gels. Both JG98 treatment and BAG3 knockdown exhibited reductions in total MyBP-C protein levels (Supplemental Figure 10, Figure 5). This work shows that disruption of BAG3 is sufficient to reduce MyBP-C protein levels.

The ability of BAG3 knockdown to reduce steady-state levels of MyBP-C has not been previously established. Yang et al<sup>48</sup> recently explored knockdown of BAG3 in iPSC-CMs, showing that reduced BAG3 leads to sarcomere damage after 10 days. The investigators performed immunofluorescence and Western blot analysis to evaluate MyBP-C protein levels and found mild reductions by immunofluorescence but no change according to Western blot. It is possible that the shorter time points of 24 hours after JG98 treatment or 96 hours of shRNA knockdown could explain this discrepancy, as modulation of chaperone effects typically results in rapid changes in protein stability, and compensation by other factors (eg, other BAG proteins) can occur at longer time points. We observed robust reductions of MyBP-C levels with BAG3 knockdown, clearly establishing this relationship.

Our work supports a growing body of evidence highlighting the importance of BAG3 in sarcomere proteostasis. The Hsp70-BAG3 protein complex can regulate clearance of client proteins via chaperone-assisted selective autophagy or the ubiquitin proteasome system.<sup>35,49,50</sup> We found that proteasome inhibition blocks the effect of JG98 to reduce MyBP-C protein levels. This is consistent with our prior work showing that MyBP-C is cleared through the proteasome and not through autophagic pathways.<sup>6</sup> Future studies examining the effects of JG98 or BAG3 knockdown on the ubiquitination state of MyBP-C, as well as the involvement of other co-chaperones and ubiquitin ligases in its degradation, will be critical for understanding how these protein interactions can be leveraged for therapeutic benefit.

It is important to highlight that JG98 treatment is not a therapeutic strategy, as JG98 decreases MyBP-C protein levels, which is the opposite direction of effect desired for a therapy targeting HCM caused by MyBP-C haploinsufficiency. Interestingly, we also observed that JG98 inhibited contractility. The effect of JG98 on contractility is likely independent of its effect on MyBP-C because complete knockout of MyBP-C exhibits a more subtle decrease in fractional shortening and increases normalized contraction.<sup>15,19</sup> This result could be due to other pleiotropic effects of JG98 or reflect the effect of JG98 on other clients of the Hsp70-BAG3 complex.<sup>34</sup> Thus, JG98 is not a therapeutic lead but rather helped to uncover the Hsp70-BAG3 axis as a high-priority focus area for future studies. For example, therapeutic strategies that enhance the formation of an Hsp70-BAG3 complex may increase MyBP-C protein levels. This may include adeno-associated virus-mediated overexpression of BAG3.

**STUDY LIMITATIONS.** First, our studies were performed in iPSC-CMs. Performing a high-throughput screen of this nature would not be possible without the use of iPSC-CMs. Nonetheless, iPSC-CMs exist in an immature state compared with adult cardiac myocytes. Thus, future studies will be needed to evaluate the role of BAG3 in more mature model systems. Second, the absence of haploinsufficiency in iPSC-CM cellular models is an important limitation.<sup>15,51</sup> Identifying iPSC-CM models that exhibit haploinsufficiency and functional phenotypes, such as hypercontractility, will be important to successfully leveraging these cellular models to identify therapeutic leads. Furthermore, we acknowledge the limitations of compounds identified in our study. Both PTL and JG98 have poor potency, which limits their utility as chemical probes. Likewise, PTL has many known targets, and JG98 modulates the function of Hsp70, a chaperone that acts on multiple cellular client proteins. Future work will be needed to understand the broader effects of these compounds on the proteome. Also, although JG98 did not have significant toxicity or effects on myofibrillar disarray at concentrations that reduced MyBP-C protein levels, it did result in reductions in MYH levels and cardiotoxicity at approximately 1.5- to 3-fold higher doses and inhibited contraction in iPSC-CMs. These findings limit its applications as a chemical probe in

cardiomyocytes.<sup>37</sup> Finally, although both JG98 and PTL activity was observed across both female and male iPSC-CM cell lines, this study was not designed to robustly address sex-specific differences in MyBP-C protein quality control. This remains an important future area of investigation.

## CONCLUSIONS

By screening known, biologically active compounds in an iPSC-CM model, we identified the Hsp70-BAG3 complex as an intervenable target to directly modulate MyBP-C homeostasis. These results suggest that therapies which stabilize Hsp70-BAG3 interactions or increase BAG3 protein levels may be beneficial in HCM caused by pathogenic *MYBPC3* variants.

**ACKNOWLEDGMENTS** The authors acknowledge Samantha Harris (University of Arizona) for providing the C5-C7 MyBP-C antibody. They also acknowledge Christine L. Mummery (Leiden University) for providing the patient-derived induced pluripotent stem cell line *MYBPC3* Patient1 and Jack M. Parent (University of Michigan) and Kevin Ess (Vanderbilt University) for providing the induced pluripotent stem cell line Ctrl-3 iPSC. They acknowledge the Center for Chemical Genomics staff, in particular director Andrew Alt, PhD, and Aaron Robida, PhD, and Nick Santoro, PhD, for guidance and technical support.

## FUNDING SUPPORT AND AUTHOR DISCLOSURES

This project was funded in part by a grant from the Center for Chemical Genomics at the University of Michigan. Dr Thompson is supported by the National Institutes of Health/National Heart, Lung, and Blood Institute (NIH/NHLBI) (T32 HL007853, K08HL163328). Dr Thompson is also supported by the Protein Folding Disease Initiative and Michigan Biology of Cardiovascular Aging (M-BoCA) at the University of Michigan. Dr Day is supported by the NIH/NHLBI (HL155568), University of Pennsylvania discretionary funding, and a Presidential Professorship. Dr Wagner is supported by an NIH T32

(T32 AR053461) training grant award to the Penn Muscle Institute. Dr Gestwicki is supported by the NIH (NS059690). Dr Ginsburg is a Howard Hughes Medical Institute Investigator and is also supported by the NIH/NHLBI (R35-HL135793). Dr Thompson has received compensation as editor for *Merck Manuals*. Dr Day is a consultant for Bristol Myers Squibb, Tenaya Therapeutics, and Pfizer. Drs Day and Helms receive support from Bristol Myers Squibb and Pfizer for the SHaRe registry (Sarcomeric Human Cardiomyopathy Registry). Dr Day has received research funding from Lexicon Pharmaceuticals. Dr Helms is a consultant for Tenaya Therapeutics and LEXEO Therapeutics. Dr Gestwicki is a co-founder of Kaizen Therapeutics and a consultant for Faze, Contour, DICE therapeutics, and Protego Biopharma. Dr Ginsburg benefits from patent royalties from Takeda to Boston Children's Hospital (von Willebrand factor) and the University of Michigan (ADAMTS13) and is a consultant for Equilibra Bioscience. These entities had no role in the preparation of the data presented or approving content of these data. All other authors have reported that they have no relationships relevant to the contents of this paper to disclose.

**ADDRESS FOR CORRESPONDENCE:** Dr Andrea D. Thompson, University of Michigan Medical School, Department of Internal Medicine, Division of Cardiovascular Medicine, 1150 W Medical Center Drive, 7220B Medical Science Research Building III, Ann Arbor, Michigan 48109, USA. E-mail: [adooley@med.umich.edu](mailto:adooley@med.umich.edu). [@dooley\\_phd](https://twitter.com/dooley_phd).

## PERSPECTIVES

**COMPETENCY IN MEDICAL KNOWLEDGE:** HCM is commonly caused by pathogenic *MYBPC3* variants that reduce total levels of WT MyBP-C protein. However, the pathways that regulate MyBP-C protein levels are poorly understood. By screening biologically active compounds in an iPSC-CM model, this study identified the Hsp70-BAG3 complex as a key regulator of MyBP-C protein levels.

**TRANSLATIONAL OUTLOOK:** These results suggest that therapeutically targeting stabilization of the Hsp70-BAG3 interactions or increasing BAG3 protein levels may be beneficial in HCM caused by pathogenic *MYBPC3* variants.

## REFERENCES

1. Ho CY, Day SM, Ashley EA, et al. Genotype and lifetime burden of disease in hypertrophic cardiomyopathy: insights from the Sarcomeric Human Cardiomyopathy Registry (SHaRe). *Circulation*. 2018;138:1387-1398.
2. Walsh R, Thomson KL, Ware JS, et al. Reassessment of Mendelian gene pathogenicity using 7,855 cardiomyopathy cases and 60,706 reference samples. *Genet Med*. 2017;19:192-203.
3. Helms AS, Thompson AD, Day SM. Translation of new and emerging therapies for genetic cardiomyopathies. *J Am Coll Cardiol Basic Trans Science*. 2022;7:70-83.
4. Helms AS, Thompson AD, Glazier AA, et al. Spatial and functional distribution of MYBPC3 pathogenic variants and clinical outcomes in patients with hypertrophic cardiomyopathy. *Circ Genom Precis Med*. 2020;13:396-405.
5. Vignier N, Schlossarek S, Fraysse B, et al. Nonsense-mediated mRNA decay and ubiquitin-proteasome system regulate cardiac myosin-binding protein C mutant levels in cardiomyopathic mice. *Circ Res*. 2009;105:239-248.
6. Glazier AA, Hafeez N, Mellacheruvu D, et al. HSC70 is a chaperone for wild-type and mutant cardiac myosin binding protein C. *JCI Insight*. 2018;3:e99319.

7. O'Leary TS, Snyder J, Sadayappan S, Day SM, Previs MJ. MYBPC3 truncation mutations enhance actomyosin contractile mechanics in human hypertrophic cardiomyopathy. *J Mol Cell Cardiol.* 2019;127:165-173.
8. Glazier AA, Thompson A, Day SM. Allelic imbalance and haploinsufficiency in MYBPC3-linked hypertrophic cardiomyopathy. *Pflugers Arch.* 2019;471:781-793.
9. Marston S, Copeland O, Jacques A, et al. Evidence from human myectomy samples that MYBPC3 mutations cause hypertrophic cardiomyopathy through haploinsufficiency. *Circ Res.* 2009;105:219-222.
10. Barefield D, Kumar M, Gorham J, et al. Haploinsufficiency of MYBPC3 exacerbates the development of hypertrophic cardiomyopathy in heterozygous mice. *J Mol Cell Cardiol.* 2015;79:234-243.
11. Monteiro da Rocha A, Guerrero-Serna G, Helms A, et al. Deficient cMyBP-C protein expression during cardiomyocyte differentiation underlies human hypertrophic cardiomyopathy cellular phenotypes in disease specific human ES cell derived cardiomyocytes. *J Mol Cell Cardiol.* 2016;99:197-206.
12. Prondzynski M, Kramer E, Laufer SD, et al. Evaluation of MYBPC3 trans-splicing and gene replacement as therapeutic options in human iPSC-derived cardiomyocytes. *Mol Ther Nucleic Acids.* 2017;7:475-486.
13. Prondzynski M, Mearini G, Carrier L. Gene therapy strategies in the treatment of hypertrophic cardiomyopathy. *Pflugers Arch.* 2019;471:807-815.
14. Mearini G, Stimpel D, Geertz B, et al. Mybpc3 gene therapy for neonatal cardiomyopathy enables long-term disease prevention in mice. *Nat Commun.* 2014;5:5515.
15. Helms AS, Tang VT, O'Leary TS, et al. Effects of MYBPC3 loss-of-function mutations preceding hypertrophic cardiomyopathy. *JCI Insight.* 2020;5:e133782.
16. Dambrot C, Braam SR, Tertoolen LG, Birket M, Atsma DE, Mummery CL. Serum supplemented culture medium masks hypertrophic phenotypes in human pluripotent stem cell derived cardiomyocytes. *J Cell Mol Med.* 2014;18:1509-1518.
17. Birket MJ, Ribeiro MC, Kosmidis G, et al. Contractile defect caused by mutation in MYBPC3 revealed under conditions optimized for human PSC-cardiomyocyte function. *Cell Rep.* 2015;13:733-745.
18. Tidball AM, Bryan MR, Uhouse MA, et al. A novel manganese-dependent ATM-p53 signaling pathway is selectively impaired in patient-based neuroprogenitor and murine striatal models of Huntington's disease. *Hum Mol Genet.* 2015;24:1929-1944.
19. Tsan YC, DePalma SJ, Zhao YT, et al. Physiologic biomechanics enhance reproducible contractile development in a stem cell derived cardiac muscle platform. *Nat Commun.* 2021;12:6167.
20. Freund RRA, Gobrecht P, Fischer D, Arndt HD. Advances in chemistry and bioactivity of parthenolide. *Nat Prod Rep.* 2020;37:541-565.
21. Robison P, Caporizzo MA, Ahmadzadeh H, et al. Detyrosinated microtubules buckle and bear load in contracting cardiomyocytes. *Science.* 2016;352:aaf0659.
22. Shin M, McGowan A, DiNatale GJ, Chiramanewong T, Cai T, Connor RE. Hsp72 is an intracellular target of the alpha,beta-unsaturated sesquiterpene lactone, parthenolide. *ACS Omega.* 2017;2:7267-7274.
23. Li X, Colvin T, Rauch JN, et al. Validation of the Hsp70-Bag3 protein-protein interaction as a potential therapeutic target in cancer. *Mol Cancer Ther.* 2015;14:642-648.
24. Li X, Shao H, Taylor IR, Gestwicki JE. Targeting allosteric control mechanisms in heat shock protein 70 (Hsp70). *Curr Top Med Chem.* 2016;16:2729-2740.
25. Dominguez F, Cuenca S, Bilinska Z, et al. Dilated cardiomyopathy due to BLC2-associated athanogene 3 (BAG3) mutations. *J Am Coll Cardiol.* 2018;72:2471-2481.
26. Martin TG, Tawfik S, Moravec CS, Pak TR, Kirk JA. BAG3 expression and sarcomere localization in the human heart are linked to HSF-1 and are differentially affected by sex and disease. *Am J Physiol Heart Circ Physiol.* 2021;320:H2339-H2350.
27. Shao H, Li X, Moses MA, et al. Exploration of benzothiazole rhodocyanines as allosteric inhibitors of protein-protein interactions with heat shock protein 70 (Hsp70). *J Med Chem.* 2018;61:6163-6177.
28. Ouimet CM, Shao H, Rauch JN, et al. Protein cross-linking capillary electrophoresis for protein-protein interaction analysis. *Anal Chem.* 2016;88:8272-8278.
29. Miyata Y, Li X, Lee HF, et al. Synthesis and initial evaluation of YM-08, a blood-brain barrier permeable derivative of the heat shock protein 70 (Hsp70) inhibitor MKT-077, which reduces tau levels. *ACS Chem Neurosci.* 2013;4:930-939.
30. Li X, Srinivasan SR, Connarn J, et al. Analogs of the allosteric heat shock protein 70 (Hsp70) inhibitor, MKT-077, as anti-cancer agents. *ACS Med Chem Lett.* 2013;4:1042-1047.
31. Aillaud C, Bosc C, Peris L, et al. Vasohibins/SVBP are tubulin carboxypeptidases (TCPs) that regulate neuron differentiation. *Science.* 2017;358:1448-1453.
32. Nieuwenhuis J, Adamopoulos A, Bleijerveld OB, et al. Vasohibins encode tubulin detyrosinating activity. *Science.* 2017;358:1453-1456.
33. Janke C, Bulinski JC. Post-translational regulation of the microtubule cytoskeleton: mechanisms and functions. *Nat Rev Mol Cell Biol.* 2011;12:773-786.
34. Judge LM, Perez-Bermejo JA, Truong A, et al. A BAG3 chaperone complex maintains cardiomyocyte function during proteotoxic stress. *JCI Insight.* 2017;2:e94623.
35. Martin TG, Myers VD, Dubey P, et al. Cardiomyocyte contractile impairment in heart failure results from reduced BAG3-mediated sarcomeric protein turnover. *Nat Commun.* 2021;12:2942.
36. Kirk JA, Cheung JY, Feldman AM. Therapeutic targeting of BAG3: considering its complexity in cancer and heart disease. *J Clin Invest.* 2021;131:e149415.
37. Martin TG, Delligatti CE, Muntu NA, Stachowski-Doll MJ, Kirk JA. Pharmacological inhibition of BAG3-HSP70 with the proposed cancer therapeutic JG-98 is toxic for cardiomyocytes. *J Cell Biochem.* 2022;123:128-141.
38. Liu L, Sun K, Zhang X, Tang Y, Xu D. Advances in the role and mechanism of BAG3 in dilated cardiomyopathy. *Heart Fail Rev.* 2021;26:183-194.
39. Powers MV, Clarke PA, Workman P. Dual targeting of HSC70 and HSP72 inhibits HSP90 function and induces tumor-specific apoptosis. *Cancer Cell.* 2008;14:250-262.
40. Rousaki A, Miyata Y, Jinwal UK, Dickey CA, Gestwicki JE, Zuidekerweg ER. Allosteric drugs: the interaction of antitumor compound MKT-077 with human Hsp70 chaperones. *J Mol Biol.* 2011;411:614-632.
41. Gestwicki JE, Shao H. Inhibitors and chemical probes for molecular chaperone networks. *J Biol Chem.* 2019;294:2151-2161.
42. Feldman AM, Begay RL, Knezevic T, et al. Decreased levels of BAG3 in a family with a rare variant and in idiopathic dilated cardiomyopathy. *J Cell Physiol.* 2014;229:1697-1702.
43. Ellinor PT, Sasse-Klaassen S, Probst S, et al. A novel locus for dilated cardiomyopathy, diffuse myocardial fibrosis, and sudden death on chromosome 10q25-26. *J Am Coll Cardiol.* 2006;48:106-111.
44. Villard E, Perret C, Gary F, et al. A genome-wide association study identifies two loci associated with heart failure due to dilated cardiomyopathy. *Eur Heart J.* 2011;32:1065-1076.
45. Harper AR, Goel A, Grace C, et al. Common genetic variants and modifiable risk factors underpin hypertrophic cardiomyopathy susceptibility and expressivity. *Nat Genet.* 2021;53:135-142.
46. Tadros R, Francis C, Xu X, et al. Shared genetic pathways contribute to risk of hypertrophic and dilated cardiomyopathies with opposite directions of effect. *Nat Genet.* 2021;53:128-134.
47. Fang X, Bogomolovas J, Wu T, et al. Loss-of-function mutations in co-chaperone BAG3 destabilize small HSPs and cause cardiomyopathy. *J Clin Invest.* 2017;127:3189-3200.



48. Yang J, Grafton F, Ranjbarvaziri S, et al. Phenotypic screening with deep learning identifies HDAC6 inhibitors as cardioprotective in a BAG3 mouse model of dilated cardiomyopathy. *Sci Transl Med*. 2022;14:eabl5654.

49. Rauch JN, Gestwicki JE. Binding of human nucleotide exchange factors to heat shock protein 70 (Hsp70) generates functionally distinct complexes in vitro. *J Biol Chem*. 2014;289:1402-1414.

50. Doong H, Rizzo K, Fang S, Kulpa V, Weissman AM, Kohn EC. CAIR-1/BAG-3 abrogates heat shock protein-70 chaperone complex-mediated protein degradation: accumulation of poly-ubiquitinated Hsp90 client proteins. *J Biol Chem*. 2003;278:28490-28500.

51. Seeger T, Shrestha R, Lam CK, et al. A premature termination codon mutation in MYBPC3 causes hypertrophic cardiomyopathy via

chronic activation of nonsense-mediated decay. *Circulation*. 2019;139:799-811.

---

**KEY WORDS** BAG3, hypertrophic cardiomyopathy, molecular chaperones, MYBPC3

---

**APPENDIX** For supplemental figures and tables, please see the online version of this paper.